73rd International Astronautical Congress (IAC), Paris, France, 18-22 September 2022.

IAC-22-73308

Rapid Prototyping Atmosphinder: Kite Propulsion Rover

Erin Kennedy[a]*

[a] *Robot Missions Inc., Ottawa, Ontario, Canada*, erin@robotmissions.org
* Corresponding Author

Abstract

The south polar region of Mars is host to seasonal CO2 gas jet eruptions, which are important agents of geological change. However, an active plume occurs for 1-2 hours and is challenging to observe. Further insight is needed for relating this to Mars' climate modeling of the atmospheric system. The proposed rover, "Atmosphinder", has the science objective of observing a plume in action from the surface and aerial vantage point. Robotically controlled trim lines are connected to a solar balloon for propulsion by winds and for lift to cross crevasses. The rover glides across the ice cushioned by a layer of gas, as generated from sublimation by a heated keel. Prototype development is underway, and further testing will be conducted at the Mars Desert Research Station (MDRS). The Atmosphinder concept demonstrates the potential to gain valuable insights about environmental science from this unique geomorphic process that is unlike any on Earth.
Keywords: Mars; South Polar Cap; Mars Rover; Balloon; CO2 Ice; Sublimation;

1. Background

The south pole of Mars is home to dynamic geomorphic processes such as CO2 jets that cause eruptions of sediment.

For the CO2 jets to happen, the solid state greenhouse effect [1, 5] takes place. This occurs after the seasonal CO2 has frozen, forming an impermeable slab of translucent ice [2]. Approximately 70% of the sunlight reaches the subsurface [2, 3], which then heats up the sediment and regolith underneath, known as insolation [4]. When this happens, the thermal radiation cannot escape. The pressure is building, causing a portion of the slab to levitate [4] momentarily, until finally the ice ruptures and forms a vent [5]. A massive plume escapes from the vent containing gas and grains of sediment [5], reaching 100 m [6]. As the eruption subsides, the dust settles onto the surface in the form of fans and blotches [5].

The understanding of the CO2 jet process is known as the "Kieffer" model [2, 7, 8, 9], with information from numerous Mars instruments, primarily from the Mars Reconnaissance Orbiter (MRO) High Resolution Imaging Science Experiment (HiRISE) [2, 10].

These jets are daily active processes. Fig. 1 and Fig. 2 show 106 hours difference.

In Fig. 1 and Fig. 2, the dark fans are from the dust laying on the top of the surface. The bright blue features are the recondensed CO2 on top of the ice as fine-grained bright frost. Below the ice is the surface, with surface tone affected by the translucent ice.

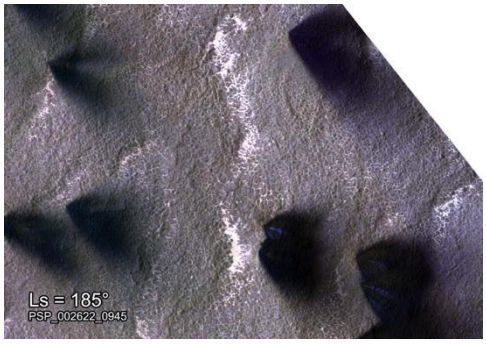

Fig. 1. Jets at Ls = 185 deg. Image credit: NASA/JPL-Caltech/UArizona [11]

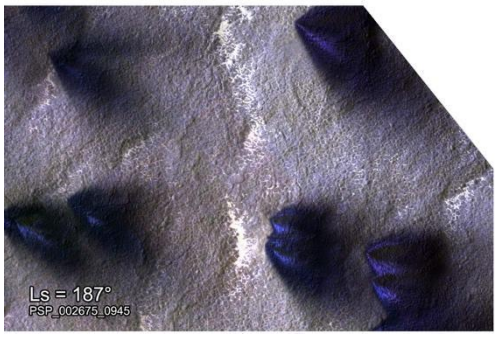

Fig. 2. Jets at Ls = 187 deg. Image credit: NASA/JPL-Caltech/UArizona [12]

The fans and blotches that speckle the region give information regarding the wind direction and speed. Citizen science efforts have led to the quantification of this [2, 6]. Fans form days to weeks later than when the spots first appear [4], and the spots repeat year after year [4, 13, 14]. The temperature of the fans are within

that of the CO2 ice temperature (~145 K) [4], compared to bare soil which warms to > 225 K within days of when the CO2 ice melts [4, 15, 16].

The surface is also host to a feature called araneiforms [5]. These spider-like features form large troughs, with the central depression of the araneiform spanning ~50 m across and the entire branches reaching up to 1 km across [5, 17, 18]. These features are carved out by erosion from the CO2 jet process. It is hypothesized that this araneiform morphology is what establishes the year to year repeatability for the spot locations [4].

Orbital studies from HiRISE on MRO have shown that winds transport fine-grained sediments across Mars [19]. This similar impact can also be seen on Earth with grains of sand being transported from the Saharan desert to the Amazon rainforest [20]. This environmental process is significant because nutrients are transported for plant proteins and growth [20] across vast distances as demonstrated by the Earth example.

To date, there have not been observations of a plume in action [5]. Current hypotheses as to why are due to the composition of the plumes: being shallow and optically thin [5], or the timing not coinciding with a HiRISE flyby. Observing plumes in action, along with performing additional science tasks to validate the hypothesized model, would be better served by a planetary rover.

2. Region of Interest

The region of interest is Manhattan (-86.39 deg latitude, 99 deg longitude), located within the 'cryptic region' of the south pole of Mars. The smooth terrain enables quicker navigation between waypoints to explore a broader area. There is only 270 m elevation change over approximately 8 km (~ 2 deg slope) [21]. Access to a trough on the eastern side of a South Polar Layered Deposit (SPLD) would be an additional interesting place to make science observations [21].

The region was determined through a weighted matrix factoring the location, surface terrain, and presence of fans. Surface was of the greatest weighting as smoother surfaces increase the probability of mission success by lowering the risk of the rover becoming stuck. Other candidate locations included Ithaca, Giza, and Inca City.

The ideal time to land would be near the southern spring equinox at Ls = 180 deg. This means that the ice would already be frozen, and there would be an increasing amount of sunlight, thereby increasing the temperature.

The time duration from Ls = 180 deg to Ls = 260 deg is approximately 4 months.

Table 1. Mars Ls and milestone regarding activities on the south pole

Ls	Milestone
170	End of the southern polar night [6]
180	Southern spring equinox [4]
200	Araneiforms' troughs become visibly brighter [21]
223	Virtually all spots and fans have formed [4]
229	Reduction in activity [4]
245	End of spring season [22]
260	Ice disappears [4], complete sublimation of seasonal frost [6]

The temperature steadily increases from 140 K to 160 K from Ls = 170 deg to Ls = 250 deg. At Ls = 250 there is a rapid increase to a maximum temperature of 245 K near Ls = 260 deg. The temperature remains stable until Ls = 300 deg, when the temperature begins to decline [22]. This information originates from data from the Mars Odyssey Mission - Thermal Emission Imaging System (THEMIS) [23].

3. Science Objectives

There are puzzles that remain in the understanding of the CO2 gas jet process. By investigating this on the surface of Mars, the information could be validated with on the ground data.

The following science objectives would be undertaken by Atmosphinder:

1. Observe a plume in action, recording the duration, height, and apparent particle size
2. Conduct a visual survey of the debris from previously erupted jets
3. Characterize the troughs, seasonal boundary zone, and layered terrain

Activities based on these science objectives could include the following:

- Observing at different altitudes during a plume eruption to indicate different masses of the ejecta. This could be used to determine a scale of eruption strength.
- Measuring the amount of surface shake prior to an eruption. It has been hypothesized that the slab levitates then eventually ruptures. This data could lead to understanding if there are any early detection indicators prior to an eruption.
- Quantifying the number of eruptions needed to form the fans, and observing the fans change over time. This could give insight into the winds and atmospheric processes that transport

the dust. It is unconfirmed whether the dust that is deposited on the surface after an eruption also has a CO2 sublimation process that 'cleanses' the ice.

- Observing the edge of a crevasse / trough to see the composition of layers at different depths.
- Observing the seasonal boundary zone after the spring concludes. Seeing how gradually it melts, and if it does so directly from the edge or in a different formation.

Photography from the aerial view is well suited for several of these activities, as a similar technique has been used on Earth to map periglacial geomorphology for analyzing ice networks [24].

A concept rover is proposed to conduct these science objectives. The outcomes would provide a ground truth to existing satellite imagery by capturing photos from the surface and an aerial view. Development and results from early Earth-based prototype development and testing are shared.

4. Mars Rover Concept

4.1 Overview

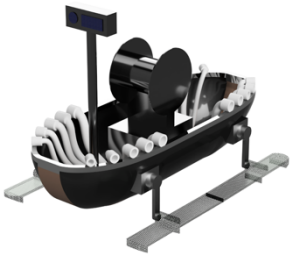

Fig. 3. Atmosphinder rover concept model

The concept explores the idea of a rover that is primarily propelled by the wind. The rover has a heated keel to generate a cushion of CO2 gas allowing it to glide over the ice. The gas is diverted away from the hull of the rover through tubing. Robotic trimmers adjust the lines to the kite / balloon, to control the tension and thus direction. A mast with a camera is used to track the position of the kite and make surface observations, along with serving as a mount for the communication antennas. Solar panels line the top surface of the rover. A gondola payload on the balloon contains a camera to conduct aerial observations of the surface.

4.2 Kite / Solar Montgolfiere Balloon

Fig. 4. Solar Montgolfiere balloon tethered to rover

The solar Montgolfiere balloon creates buoyancy by having a different internal envelope temperature to external temperature. The heat is generated from the sun heating the material of the balloon. The Atmosphinder concept Montgolfiere solar balloon serves dual purpose as a kite and a balloon. The kite is needed to tow the rover, and the balloon is needed to lift the rover over crevasses.

The Montgolfiere balloons have been tested before. At the the French Centre National d'Etudes

Spatiales (CNES) balloons have been flown for periods of 69 days [25, 26] in Earth's upper stratosphere, which is similar to the Martian atmosphere. As well, NASA's Jet Propulsion Laboratory (JPL) has tested balloons [25], one of which included a vent to control altitude [25, 27].

These balloons have the advantage of long duration flight, such as an estimated 1-2 months at the Mars poles [28]. Another key advantage being that small holes resulting in leaking air do not adversely affect the solar balloon [29]. For landing, it has been estimated that balloons with payloads could be landed with less than 1% of the vertical energy as opposed to parachutes [25].

Following a model, a 10 kg payload can be lifted by a 18 m balloon [30]. The ascent commences as soon as the internal temperature of the balloon reaches 340 K [30]. An altitude setpoint is able to be set between Martian hours 9 - 15, where the balloon oscillates around that target [30]. For a target altitude of 2000 m, there would be 3.5 hours of stable operational time [30]. If the payload is 0 kg, as in, the balloon is in steady-state operation and not lifting the rover, then the time is 6 hours of stable operational time [30]. This model is based on the surface temperature being 225 K [30]. Adjustments to the model would need to be taken into account as the temperature near south spring starts at 140 K, rising to maximum 245 K [22].

The balloon itself does not have rigidity to serve as a kite. To do so, the design of the balloon would have supportive leading ribs, similar to kite foils for surfing on the edges, extending from the top to bottom. This

rigidity would provide surface area for drag that is not significantly deformed by the winds. For future work, it would be necessary to experimentally validate that this hypothesized design would work in Mars' low atmospheric pressure.

The spreader ring on the entrance of the kite contains connection points for the robotically controlled trim lines on the rover. The vent would also be robotically controlled and have a line.

Crossing crevasses would be quite the acrobatic sight. When the rover detects a crevasse from its computer vision system, it will reel in the trim lines to lift itself off the surface, as supported by the balloon. This also poses an interesting challenge for planning throughout the mission, where there will be a heavy reliance on the autonomous navigation while journeying to reach waypoints.

4.3 Wind Propulsion

With the lines being adjustable with robotic trimmers, tension can be adjusted, and direction can be controlled. The winds on Mars could pull the kite, and through tension in the lines, this could push the surface payload. With reduced friction from the locomotion system, this makes pushing even easier. Winds are estimated to range from 1 m/s to 9 m/s in the Manhattan region of Mars [6].

4.4 Locomotion

Fig. 5. Underneath the rover, showing the keel line and channels for gas to move through

The same process of the CO2 jets can be advantageous for locomotion. When CO2 sublimates, it changes into a gas. This gas could be used to form a cushion between the hull, allowing the rover to glide with less friction. The keel of the rover is copper, and would be heated to increase the surface temperature by 20 K. This would result in the CO2 ice reaching its sublimation point.

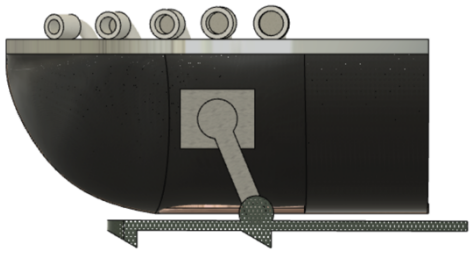

Fig. 6. Side view of rover showing the ski position when in contact with the surface

The method of driven locomotion is a four bar linkage with a motorized arm. The longest linkage that remains parallel to the ground is referred to as the 'ski'. When revolving, the ski makes contact with the surface. Teeth on the ski, akin to an ice pick, grip to push the rover forward. To move straight, the left and right side skis alternate pushing. When at rest, the skis can return to their upright parked position, and the rover would be resting on its keel. This reduces the risk of the skis becoming frozen to the surface.

4.5 Mast

The mast of the rover contains the camera needed for computer vision in the visual spectrum. The camera is housed in a heated box. Using a pan-tilt servo mechanism, the camera tracks the position of the kite, and performs surface observations. Antennas for communication to Earth and orbiting relays are mounted onto the mast.

4.6 Internal Hull

Inside the hull are the rover's electronics for its embedded system controller, the line trimmers, thermal regulation control, and power management. The internal hull box is heated with the use of radioisotope heater units (RHU). On the top surface of the hull are solar panels.

4.7 Gondola Payload

The gondola payload is external to the rover and attached to the entrance ring of the balloon. Pointed down, it contains a camera in the visual spectrum to conduct aerial observations.

4.8 Requirements & Constraints

The maximum mass is 10 kg. The concept mass distribution is as follows in Table 2.

Table 2. Mass budget of concept rover

Component	Mass (kg)	Percent of Total
Batteries	3	30.00%
Solar panels	1.5	15.00%
Structure	3	30.00%
Motors, Electronics, Sensors	2	20.00%
Gondola Camera	0.5	5.00%
Total	**10**	**100.00%**

5. Rover Prototype

5.1 Requirements & Constraints

As this rover is bound for an experiment at the Mars Desert Research Station (MDRS), the constraints are based on that of traveling.

The size available to the disassembled rover is within a 55 L hiking backpack, approximate internal dimensions of 74 cm x 35 cm x 28 cm. The maximum weight limit is 22 kg. After the weight of the pack, the amount remaining available for the rover is 20 kg.

The power provided to the rover is a 4S 16.8 V 2500 mAh lithium ion battery.

Based on these requirements, the design of the rover must be modular and with interlocking pieces. Fortunately, these requirements lend themselves well to the rapid prototyping approach.

5.2 Kite Control Software

Fig. 7. Kite View software developed by Robot Missions Inc [31]

Kite View is software with a user interface to monitor the tracking of the kite and control the trim lines to the kite.

The computer vision system detects the position of the kite through multiple filters. Hue filter is used first to detect the colours that are the same as the kite, resulting in a list of coordinates. From there, blobs are formed from neighbouring coordinates within a certain diameter threshold. The largest blob is assumed to be the kite.

Future functionality includes determining where to move the kite based on the target location, and sending commands to the rover's microcontroller to move the trim motors.

The software is built on the Processing.org environment [32] and uses the controlP5 [33] and OpenCV [34] libraries.

5.3 Design

An initial simplified prototype was developed in order to conduct an experiment. The design of this rover was a dual-wheel device. The kite line is attached to a freely rotating collar on the axle between the two wheels. The kite was a single-lined kite of uniform red colour for ease of computer vision tracking with the software.

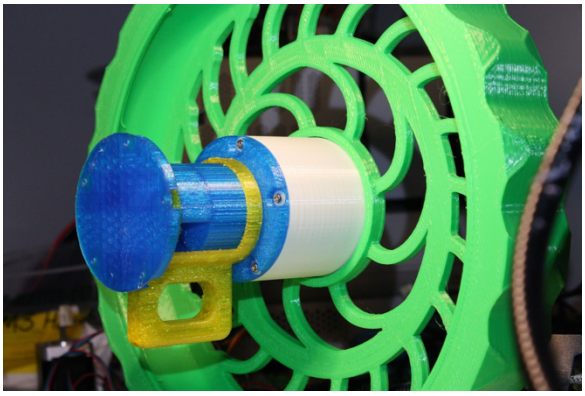

Fig. 8. Prototype for experiment with one wheel removed.

The pieces were 3D printed in polylactic acid (PLA) plastic. The wheel measures ~30 cm in diameter. The yellow piece is the collar that the kite line is connected to.

The major goal for the next design revision is the trim line control mechanism. A dual-lined kite will be used to give more control over the direction and movements.

5.4 Experiment

An initial experiment was conducted to test the hypothesis of a rover being propelled by the wind using a kite. Data from the experiment was used to test the software as well.

The prototype was placed on the grass. The windspeed was 20 km/h. The kite pulled the wheels, and was able to change directions depending on the wind direction. The software worked for tracking the position of the kite.

Fig. 9. Dual wheel prototype pulled by single-lined kite

The experiment result proved the hypothesis to be true.

Criteria for future experiments with advanced versions of the prototype will include:

1. Travel forwards
2. Turn
3. Travel backwards
4. Hold stationary

Holding a stationary position would be a combination of movements, but not venturing past a certain point. The accuracy of the criteria will serve as a baseline between experiments in order to track the performance of the prototypes.

6. Kite Modes

6.1 Overview

Fig. 10. Flying kite performing a figure-eight movement as tracked in Kite View

The kite can be controlled to have different modes. Fig. 10 above shows the test kite performing a figure-eight movement. There are several modes that will be key to the rover conducting its activities. These modes are currently in active development and are suited for both the Earth prototype and the Mars Atmosphinder concept.

6.2 Towing

In this mode, the kite is towing the rover across the surface. The robotic trim lines are controlled to steer the direction of the kite / balloon. The keel of the rover is heated to cause sublimation of the CO2 ice to allow a cushion of gas to glide on. The locomotion skis are parked in their upright position. The kite must be ahead of the rover, and winds must be of sufficient speed.

6.3 Steady-State

The kite / balloon is being flown but is not pulling the rover. The balloon is oscillating at its target altitude. In this mode, the gondola payload may be acquiring images. The robotic trim lines are controlled to keep the kite near a target position. The locomotion skis are in use to move the rover when necessary.

6.4 Jump

The rover is airborne and being moved by the kite / balloon. The robotic trim lines reeled the rover upwards off the surface. This requires coordination with the locomotion skis to leverage the rover, reducing the amount of area contact with the surface. While airborne, the rover can adjust the trim lines to attempt to adjust the kite / balloon direction. When the gondola camera detects a safe landing location, the rover can lower itself to the surface.

6.5 Launch & Ascent

Launch involves coordination between the robotic trim lines reeling in the lines and the locomotion skis lurching forwards. Launch can only be conducted during the operational hours of the balloon due to the required temperature. The aim of the rover movements is to create a ripple near the entrance ring of the balloon such that it can catch some wind internally into the balloon. Repeating this process would enable the internal envelope air to increase temperature. Ascent is primarily dependent on the temperature and the vent control. Further experimental work with automated launch of a kite will improve this sequence of movements.

6.6 Descent & Landing

During descent, the rover lets loose the lines while traveling a safe distance away from the kite. The distance could be up to the diameter of the kite, 18 m. This is in order for the balloon to not land on top of the rover. Daily mission planning would be needed to ensure adequate runway for safe landing of the balloon. Once the balloon is landed, the rover would be able to explore as far as the tether lines allow, akin to a dog on a leash. It would not be recommended for the rover to drag the kite, for risk of ripping the thin material.

7. Applicability to Other Planets

This concept could be applicable to missions on other planets as well.

Triton, Neptune's moon, is also host to geyser-like eruptions, as discovered by images from Voyager 2. The pressurization of Nitrogen ice from solar heating is what converts it to Nitrogen gas, and is the underlying operation of the geysers [35]. These are on quite a larger scale than the ones seen on Mars, with the plumes rising to 8 km of radii ranging several tens of meters to 1 km, and the expelled dust drifting over 100 km [35]. A temperature increase of only 4 K above ambient surface is needed to drive the plumes [35]. However, the vastly colder temperatures and thinner atmospheric pressure would need to be taken into consideration.

Applying the concept of the robotically controlled solar Montgolfieres kite, this could be used for flights above the clouds on Venus in short durations, and Jupiter and Saturn in longer durations [37].

Titan, the largest moon of Saturn, hosts an atmosphere that is approximately four times Earth's surface atmosphere. This would be an ideal location for Atmosphinder's robotically controlled kite, as even a small balloon could lift a heavy payload to a high altitude [36].

Finally, there is applicability on Earth as well for exploring the arctic regions.

8. Future Work

There are several areas of Atmosphinder that could be explored as advanced concepts:

1. Balancing the design of the Motgolfiere balloon to add rigidity while keeping it lightweight would need to be experimentally tested for performance in Mars' low atmospheric pressure.
2. At a scale model size, experimentally observing the reduced friction and flow of gas that occurs as the rover sublimates CO2 when heated by the keel.
3. Kite control algorithms for achieving different modes of operation during varying environmental conditions.

For the prototype, the next step is to prepare for the upcoming MDRS mission in 2023. This includes updating the design to be a more all-encompassing rover, implementing autonomous navigation, designing an all-in-one custom circuit board, and improving the firmware with a Real-Time Operating System (RTOS).

9. Conclusion

The dynamic south pole region of Mars has a wealth of insights waiting to be discovered which are relevant to environmental science. The proposed Atmosphinder rover concept covers a broad area while collecting data. Insights could be used for future missions that are less mobile, such as stationary landers with deep drills for ice cores. Development progress from an early Earth based prototype was shared ahead of its mission at the Mars Desert Research Station in 2023. Applicability of this concept to other planetary bodies was discussed. Ultimately, knowledge deduced from information collected by Atmosphinder could be used to better inform measures for protecting fragile environments.

References

[1] D. L. Matson, R.H. Brown, Solid-state greenhouse and their implications for icy satellites, Icarus 77 (1989) 67–81.

[2] K.M. Aye, M.E. Schwamb, G. Portyankina, C.J. Hansen, A. McMaster, G.R.M. Miller, B. Carstensen, C. Snyder, M. Parrish, S. Lynn, C. Mai, D. Miller, R.J. Simpson, A.M. Smith,
Planet Four: Probing springtime winds on Mars by mapping the southern polar CO2 jet deposits,
Icarus 319 (2019) 558-598.

[3] G.B. Hansen, Ultraviolet to near-infrared absorption spectrum of carbon dioxide ice from 0.174 to 1.8 mm, Journal of Geophysical Research 110 (2005).

[4] H. Kieffer, P. Christensen, T. Timothy, CO2 jets formed by sublimation beneath translucent slab ice in Mars' South Seasonal Polar Ice Cap, Nature 442 (2006).

[5] L. Mc Keown, J.N. McElwaine, M.C. Bourke, *et al,* The formation of araneiforms by carbon dioxide venting and vigorous sublimation dynamics under martian atmospheric pressure, Sci Rep 11 (2021).

[6] G. Portyankina, K.M. Aye, M.E. Schwamb, C.J. Hansen, T.I. Michaels,C.J. Lintott, Planet Four: Derived South Polar Martian Winds Interpreted Using Mesoscale Modeling, Earth and Space Science Open Archive (2021).

[7] C.J. Hansen, N. Thomas, G. Portyankina, A. McEwen, T. Becker, S. Byrne, K. Herkenhoff, H. Kieffer, M. Mellon, HiRISE observations of gas sublimation-driven activity in Mars' southern polar regions, Icarus 205 (2010) 283–295.

[8] H.H. Kieffer, Cold jets in the Martian polar caps, Journal of Geophysical Research 112 (2007).

[9] S. Piqueux, S. Byrne, M.I. Richardson, Polygonal Landforms at the South Pole and Implications for Exposed Water Ice, Sixth International Conference on Mars, (2003) 3275.

[10] A.S. McEwen, E.M. Eliason, J.W. Bergstrom, N.T. Bridges, C.J. Hansen, W.A. Delamere, J.A. Grant, V.C. Gulick, K.E. Herkenhoff, L. Keszthelyi, R.L. Kirk, M.T. Mellon, S.W. Squyres, N. Thomas, C.M. Weitz, Mars Reconnaissance Orbiter's High Resolution Imaging Science Experiment (HiRISE), Journal of Geophysical Research: Planets 112 (2007)

[11] C. Hansen, Active Processes: Bright Streaks and Dark Fans 12 December 2007, https://hirise.lpl.arizona.edu/PSP_002622_0945, (accessed 31.08.22) Note: See “cut_c.jpg”.
[12] C. Hansen, Active Processes: Bright Streaks and Dark Fans 12 December 2007, https://hirise.lpl.arizona.edu/PSP_002622_0945, (accessed 31.08.22) Note: See “cut_b.jpg”.
[13] B. Cantor, M. Malin, K.S. Edgett, Multiyear Mars Orbiter Camera (MOC) observations of repeated Martian weather phenomena during the northern summer season., J. Geophys. Res. 107 (2002).
[14] M.C. Malin, K.S. Edgett, Early defrosting of the 1999 south polar seasonal frost cap: Evidence of interannual climate change?, Lunar Planet. Sci. (2000).
[15] S. Piqueux, S. Byrne, M.I. Richardson, Sublimation of Mars’s southern seasonal CO2 ice cap and the formation of spiders, J. Geophys. Res. (Planets) 108 (2003).
[16] T.N. Titus, H. Kieffer, P.R. Christensen, Exposed water ice discovered near the south pole of Mars, Science 299 (2003) 1048-1051.
[17] S. Piqueux, S. Byrne, M.I. Richardson, Sublimation of Mars’s southern seasonal CO2 ice cap and the formation of spiders, J. Geophys. Res. (Planets) 108 (2003).
[18] C.J. Hansen, et al., HiRISE observations of gas sublimation-driven activity in Mars’ southern polar regions: I. Erosion of the surface, Icarus 205 (2010) 283–295.
[19] S. Silvestro, L.K. Fenton, D.A. Vaz, N.T. Bridges, G.G. Ori, Ripple migration and dune
activity on Mars: evidence for dynamic wind processes, Geophys. Res. Lett. 37 (2010).
[20] H. Yu, M. Chin, T. Yuan, H. Bian, L.A. Remer, J.M. Prospero, A. Omar, D. Winker, Y. Yang, Y. Zhang, Z. Zhang, C. Zhao, The fertilizing role of African dust in the Amazon rainforest: A first multiyear assessment based on data from Cloud-Aerosol Lidar and Infrared Pathfinder Satellite Observations, Geophys. Res. Lett. 42 (2015) 1984-1991.
[21] G. Portyankina, C.J. Hansen, K.-M. Aye, Present-day erosion of Martian polar terrain by the seasonal CO2 jets, Icarus 282 (2017) 93–103.
[22] P. Angell, P. Christensen, Seaonal Temperature Variations and CO2 Sublimation Activity Near the Martian South Pole 2018, https://spacegrant.arizona.edu/sites/spacegrant.arizona.edu/files/documents/opportunities/symposium/2018/presentations/Session%20G%20-%20Planetary%20Science/[G-02]%20Angell_Paras.pdf, (accessed 08.31.22).
[23] P.R. Christensen, B.M. Jakosky, H.H. Kieffer, M.C. Malin, H.Y. McSween, Jr., K. Nealson, G.L. Mehall, S.H. Silverman, S. Ferry, M. Caplinger, and M. Ravine, The Thermal Emission Imaging System (THEMIS) for the Mars 2001 Odyssey Mission, Space Science Reviews 110 (2004) 85-130.
[24] J. Boike, K. Yoshikawa, Mapping of periglacial geomorphology using kite/balloon aerial photography, Permafrost Periglac. Process. 14 (2003) 81-85.
[25] J. Jones, et al., Montgolfiere Balloon Missions for Mars and Titan, 3rd IPPW (2005).
[26] P. Maleterre, Long Duration Balloon Flights in the Middle Stratosphere, Adv. Space Res. Vol. 13, No. 2 (1993).
[27] J. Blamont, J. Jones, A New Method for Landing on Mars, Acta Astronautica (2002) 723-726.
[28] J. Jones, D. Fairbrother, A. Lemieux, R. Zubrin, Wind-Driven Montgolfiere Balloons For Mars (2005).
[29] J. Jones, J. Wu, Solar Montgolfiere Balloons for Mars, AIAA-LTA Conference (1999).
[30] T. Schuler, S. Shkarayev, J. Thangavelautham, Altitude Control of a Solar Balloon for Mars Exploration, Advances in the Astronautical Sciences (2020).
[31] E. Kennedy, Kite Propulsion Github Repository 6 April 2022, https://github.com/RobotGrrl/KitePropulsion, (accessed 08.31.22).
[32] Welcome to Processing, https://processing.org/, (accessed 08.31.22).
[33] A. Schlegel, controlP5 30 July 2015, https://www.sojamo.de/libraries/controlP5/, (accessed 08.31.22).
[34] G. Borenstein, opencv-processing Github Repository 21 May 2017, https://github.com/atduskgreg/opencv-processing, (accessed 08.31.22).
[35] L.A. Soderblom, S.W. Kieffer, T.L. Becker, R.H. Brown, A.F. Cook, C.J. Hansen, T.V. Johnson, R.L. Kirk, E.M. Shoemaker, Triton's Geyser-Like Plumes: Discovery and Basic Characterization, Science (1990).
[36] J.A. Jones, Inflatable Robotics for Planetary Applications, 6th International Symposium on Artificial Intelligence, Robotics, and Automation in Space (2001).